SUPPLEMENTARY DATA

CD8^{+} T-cell immune evasion enables oncolytic virus immunotherapy

Aldo Pourchet, Steven R. Fuhrmann, Karsten A. Pilones, Sandra Demaria[2],
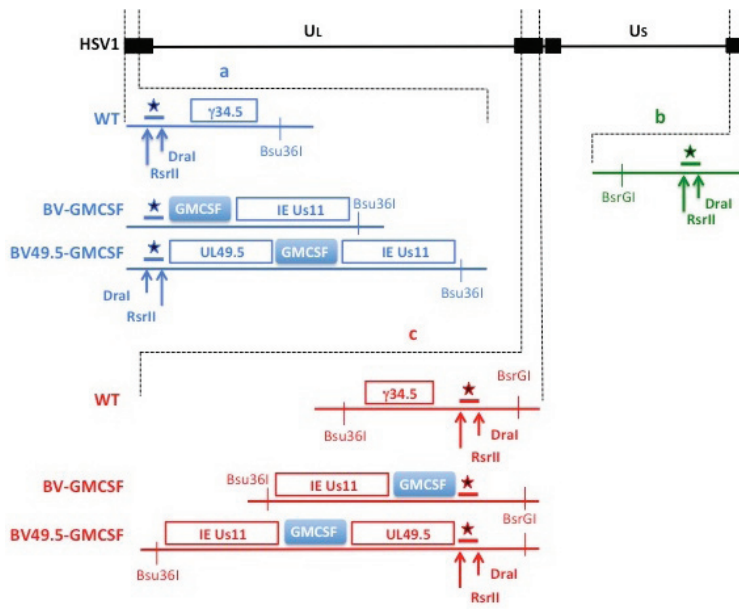
Alan B. Frey, Matthew Mulvey, & Ian Mohr

A.

HSV1 · U_L · Us

WT
★ γ34.5
DraI / RsrII / Bsu36I

b
BsrGI · ★ · DraI / RsrII

BV-GMCSF
★ GMCSF · IE Us11 · Bsu36I

BV49.5-GMCSF
★ UL49.5 · GMCSF · IE Us11
DraI / RsrII · Bsu36I

c

WT
γ34.5 · ★ · BsrGI
Bsu36I · DraI / RsrII

BV-GMCSF
Bsu36I · IE Us11 · GMCSF · ★ · BsrGI

BV49.5-GMCSF
IE Us11 · GMCSF · UL49.5 · ★ · BsrGI
Bsu36I · DraI / RsrII

B.

c - BV49.5-GMCSF
c - BV-GMCSF
c - WT
a - BV49.5-GMCSF
c - WT (long exposure)
a - BV-GMCSF
b
a - WT

10, 8, 6, 5, 4, 3, 2.5

C.

Total pfu

WT, !.34.5, SUP1, BV49.5, BV49.5-FS, BV49.5-GMCSF, BV-GMCSF

* / *** / *** / ***

D.

Total pfu

WT, !.34.5, BV49.5, BV-GMCSF
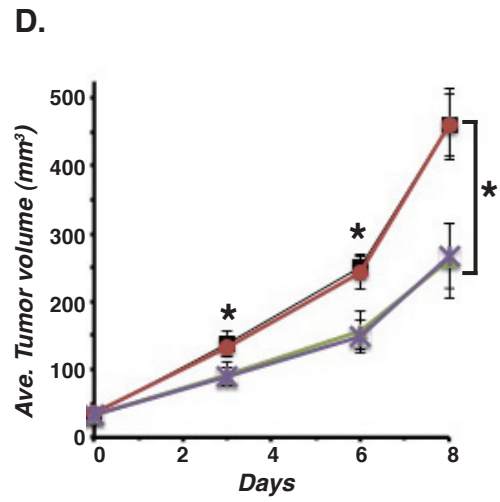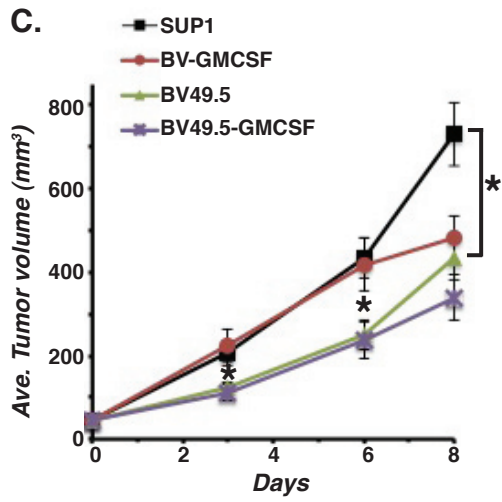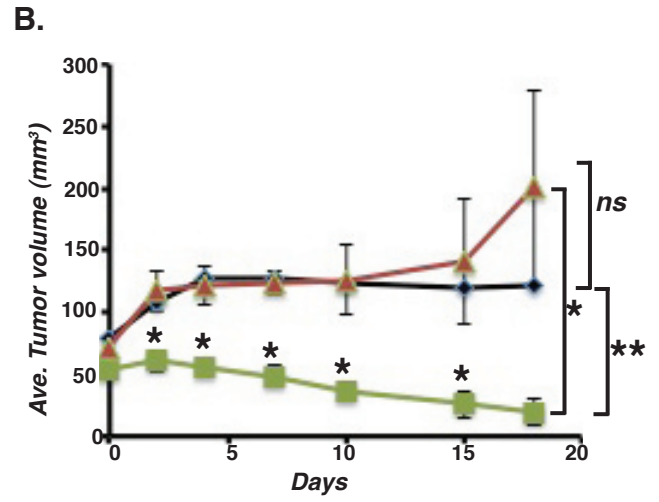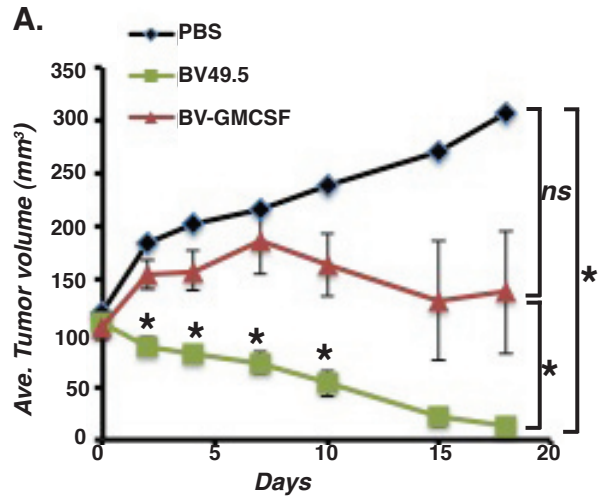
**

SUPPLEMENTAL FIGURE 1

A.

B.
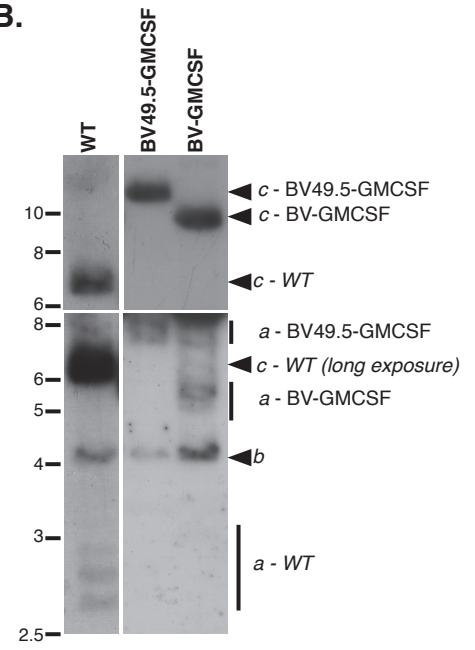
C.

D.
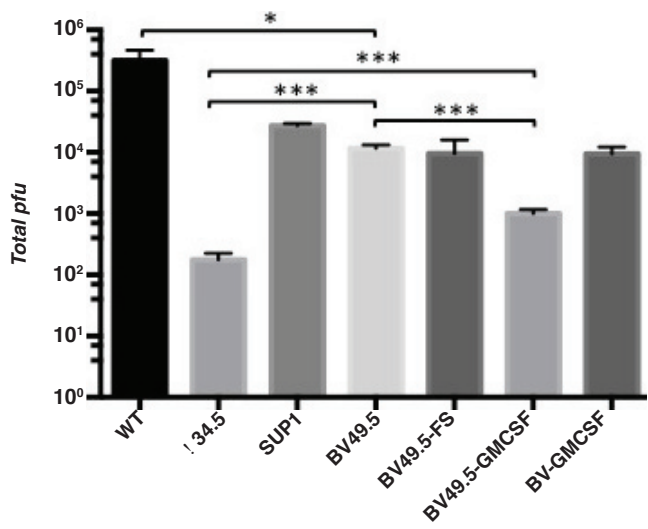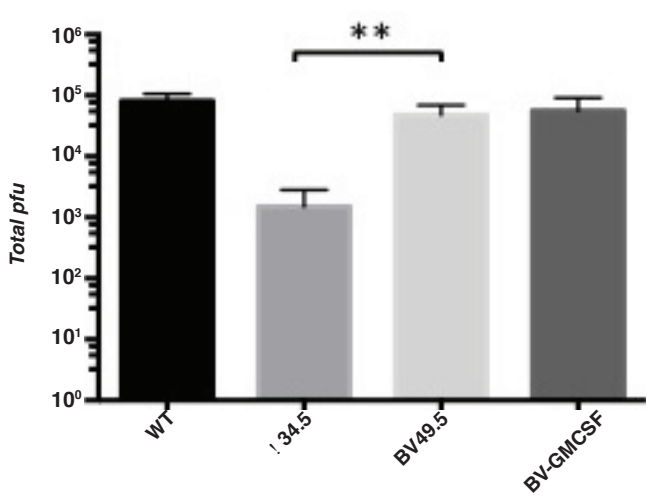
Supplemental Figure 1. Characterization of mGMCSF-expressing HSV-1 OVs compared to those only armed with IE Us11 and GMCSF. A. Physical structure of recombinant HSV-1 OV genomes expressing IE Us11 and GMCSF. The BV49.5 viral HSV-1 genome is depicted in Figure 1 of the main manuscript. The recombinant BV49.5-GMCSF expresses murine GMCSF from the HCMV major IE promoter and UL49.5 from the cellular elongation factor 1 promoter, but is otherwise identical to BV49.5. The recombinant BV-GMCSF does not contain the UL49.5 gene but is otherwise identical to BV49.5-GMCSF. The location of the ^{32}P-labeled DraI-RsrII probe and its three target sites in the genome are depicted as stars (*nucleotides 48-379 fragment a, 125987-126317 fragment c, 151910-152241 fragment b*). B. DNA isolated from virus-infected cells was doubly digested with BsrGI-Bsu36I, fractionated by electrophoresis on a 1% agarose gel, transferred to a nylon membrane and hybridized to the ^{32}P-labeled DraI-RsrII probe (depicted as a star in A). This probe identifies sequences within internal and terminal repetitive genome segments that lie outside of the !34.5 ORF. Hybridizing fragments (*a, b, c delineated in panel A*) from WT, BV49.5, BV49.5-GMCSF, and BV-GMCSF viruses are indicated on the right of the autoradiogram. The mobility of DNA molecular size standards (in Kb) is indicated on the left. Shorter (top panels) and longer (bottom panels) exposures are shown to facilitate visualization of terminal fragments that are underrepresented in replicating concatameric genomes. Intervening lanes between WT, BV49.5-GMCSF and BV-GMCSF have been spliced out. BV49.5-GMCSF and BV-GMCSF samples shown here were from the same gel as BV49.5, BV49.5-FS, and WT samples

shown in Figure 1B of the main manuscript. The WT comparator in this panel is a lighter exposure of the WT panel shown in Fig. 1B. Heterogeneity at the genomic *Bsu36I* terminal fragments is due to natural variations within a repetitive sequence component. The SUP1 HSV-1 OV, which expresses IE Us11 and cannot produce the ICP47 TAP inhibitor or mGMCSF, has been described (*1,2)*. This mutation conferring IE Us11 expression in SUP1 is equivalent to mutations introduced into clinical (T-Vec) and pre-clinical (JS1/34.5-/47/, and G47!) HSV-1 OVs (*3,4*). C. Productive virus replication in cultured murine bladder cancer cells. MBT2 (MOI= 0.02) cells were infected with the indicated virus and after 5d the amount of infectious virus present in cell free lysates was quantified by plaque assay in permissive Vero cells. As in Fig. 2d, BV49.5 and BV49.5-FS replicate equivalently. Both viruses replicate similarly to BV-GMCSF, whereas BV49.5-GMCSF replicates to approximately ten-fold reduced levels. Even though its replicative capacity is modestly reduced, BV49.5-GMCSF expresses UL49.5 and displays superior oncolytic immunotherapeutic activity compared to BV-GMCSF as shown in supplemental figure 2C,D. D. As in C except MB49 bladder cancer cells were infected (MOI=0.01) with the indicated virus. *P<0.05; **P<0.01; *** P<0.005 by student's t-test.

Supplemental Figure 2. **Superior anti-tumor efficacy of UL49.5-expressing HSV-1 OVs compared to those only armed with IE Us11 and GMCSF.** A. Tumors produced by bilateral, sc injection of MB49 mouse bladder cancer cells (*a gift from Ainhoa Perez-Diez, NIAID*) were established in left and right flanks of

C57BL/6 mice. Left flank tumors were treated by intratumoral injection (n= 9 for each group) of **BV-GMCSF** (9 x 10^6 pfu), **BV49.5** (1.5 x 10^6 pfu), or **PBS** on days 0, 2, and 4. Injected (treated) tumors were measured on the indicated days and the average tumor volume on each day plotted. Error bars reflect the SEM. In OV-treated tumors, **BV49.5** was more effective than **PBS** (*P<0.02 on day 2,4, 7; P< 0.025 on day 10; P<0.05 on day 15,18*) and more effective than **BV-GMCSF** (*P< 0.003 on day 2,4,7,10; P< 0.05 on day 18*). In addition, **BV-GMCSF** was not significantly different (ns) compared to PBS-treated tumors for all time points tested. B. As in (A) except contralateral (right flank), untreated tumor volume was plotted. **BV49.5** was more effective than **PBS** (*P<0.05 on day 2; P≤ 0.004 on day 4,7,10; P<0.05 on day 15,18*) and **BV-GMCSF** (*P< 0.007 on day 2,4,7,10; P≤ 0.04 on day 15,18*). **BV-GMCSF** was not significantly different (ns) compared to **PBS**-treated tumors for all time points tested.

The rapid antitumor activity of BV49.5 treatment in injected tumors (*Supplemental Fig. 2A*) likely results from multiple effectors including direct virus oncolysis of tumor cells and/or activation of innate antitumor immune responses. In addition, we believe the response of treated (*Supplemental Fig. 2A*) and untreated, contralateral MB49 tumors (*Supplemental Fig. 2B*) in the absence of an observable time lag for adaptive responses reflects a well-established, natural adaptive immune response against MB49 tumor cells stimulated at the time of injection (*5*). The MB49 model is one of two major murine bladder cancer models. Implantation of MB49 tumor cells, which are derived from male mice, into females allows the male HY antigen to be used, in effect, as a surrogate tumor

antigen. Indeed, a robust, T-cell containing immune infiltrate exists in untreated MB49 tumors (*5*). Significantly, this property of the MB49 model mimics observations in human tumors known to have immune infiltrates within the tumor microenvironment prior to treatment. Many of these human tumors respond to immune checkpoint inhibitor blockade therapy.

C. Bilateral, sc MBT2 mouse bladder cancer tumors were established in left and right flanks of C3H/HeN mice. Left flank tumors were treated by intratumoral injection (n= 12 for each group) of **SUP1**, **BV-GMCSF**, **BV49.5**, or **BV49.5-GMCSF** on days 0,3, and 6 (9 x10^5 pfu per injection). Tumors were measured on the indicated days and the average tumor volume on each day plotted. Error bars reflect the SEM. In OV-treated tumors, **BV49.5** was more effective than **SUP1** at all time points *(P$\leq$ 0.02 on day 3; P< 0.01 on day 6,8)* and more effective than **BV-GMCSF** on days 3 and 6 *(P<0.03)*. In addition, **BV49-GMCSF** was more effective than **BV-GMCSF** *(P$\leq$ 0.03 on days 3 and 6; P=0.086 on day 8)*. D. As in (C) except contralateral (right flank), untreated tumor volume was plotted. **BV49.5** and **BV49.5-GMCSF** were more effective than **SUP1** and **BV-GMCSF** *(P$\leq$ 0.02 on day 8; P$\leq$ 0.03 on day 6)*. On day 3, **BV49.5-GMCSF** was more effective than **BV-GMCSF** *(P<0.04)*. Strain-dependent vigor of adaptive immune responses in the two different mouse strains used in panels A,B compared to C,D likely accounts for variability in the magnitude of treatment effects.

SUPPLEMENTAL REFERENCES

1) Mohr I, Gluzman Y. (1996) A herpesvirus genetic element which affects translation in the absence of the viral GADD34 function. *EMBO J* **15:** 4759-4766.

2) Taneja S, MacGregor J, Markus S, Ha S, Mohr I (2001) Enhanced antitumor efficacy of a herpes simplex virus mutant isolated by genetic selection in cancer cells. *Proc Natl Acad Sci USA* **98**: 8804-8808.

3) Todo T, Martuza RL, Rabkin SD, Johnson PA (2001) Oncolytic herpes simplex virus vector with enhanced MHC class I presentation and tumor cell killing. *Proc. Natl. Acad. Sci. USA* **98:** 6396-6401.

4) Liu BL et al. (2003) ICP34.5 deleted herpes simplex virus with enhanced oncolytic, immune stimulating, and anti-tumour properties. *Gene Ther* **10**: 292-303.

5) Biot C et al. (2012) Preexisting BCG-specific T cells improve intravesical immunotherapy for bladder cancer. *Sci Transl Med*. **4**: 137ra72. doi: 10.1126/scitranslmed.3003586.

Supplemental Table 1. Student's t-test analysis comparing different treatments of directly injected and untreated MBT2 tumors

Directly-injected tumors

	0.1408	**0.0048**	**0.0338**
	0.0017	**0.0000**	**0.0011**
	0.0450	**0.0021**	**0.0340**
	0.0070	**0.0000**	**0.0027**
	0.0377	**0.0000**	**0.0012**

Untreated, contralateral tumors

	0.0013	**0.0123**	0.8311
	0.0007	**0.0002**	0.8563
	0.0076	**0.0038**	0.7022
	0.0076	**0.0015**	0.5634
	0.0116	**0.0115**	0.4843

Mice with bilateral, sc MBT2 tumors were established and treated as described in Figure 3. P-values for each comparison in directly-injected (top) and untreated, contralateral (bottom) were derived by multiple t-test analysis performed for each group on the indicated day. Values in **bold** were deemed significant (P<0.05).

Supplemental Table 2. Student's t-test analysis comparing different treatments of 4T1 tumors

Treated tumors

Days	BV49.5 vs BV49.5-FS	BV49.5 vs Mock	BV49.5-FS vs Mock
3	**0.0018**	**0.0106**	0.2995
6	**0.0000**	**0.0021**	0.0963
8	**0.0038**	**0.0012**	0.1806
10	**0.0008**	**0.0009**	0.0904
13	**0.0016**	**0.0002**	**0.0175**
15	**0.0002**	**0.0001**	**0.0072**
17	**0.0004**	**0.0003**	**0.0143**
20	**0.0048**	**0.0002**	**0.0053**

Treated tumors in CD8$^+$-depleted mice

Days	BV49.5 vs BV49.5-FS	BV49.5 vs Mock	BV49.5-FS vs Mock
3	0.3141	**0.0185**	0.1788
6	0.5715	0.1178	0.4421
9	0.8883	**0.0311**	0.0630
13	0.9913	**0.0107**	**0.0040**
16	0.8208	0.0739	**0.0264**
20	0.9769	0.7550	0.8025

Mice with sc 4T1 tumors were established and treated as described in Figure 4. P-values for each comparison in treated tumors (top) and treated tumors in CD8$^+$-depleted mice (bottom) were derived by multiple t-test analysis performed for each group on the indicated day. Values in **bold** were deemed significant (P<0.05).